

Friction Stir Welding Process and Chemical Properties Analysis of AZ80 Magnesium Alloy Material

Wenhui Yang, Lijun Xie*

Changsha Vocational & Technical College, Changsha 410111, China
 xlj0209@163.com

Research on friction stir welding temperature field, welding heat transfer, thermal cycling process and weld nugget formation was important for welding structure reliability and safety. At present, the domestic and foreign studies about FSW mainly concentrated in the welding process, welding materials, microstructure and mechanical properties of joint of friction stir head mechanism. The results of finite element calculated in this paper, the data in the file storage format was chose for research, the design data is read from the algorithm and realizes the extraction of different types of data. This paper uses the element local stress polishing and method for smoothing, the Gauss integral point welding stress numerical conversion data, laid the foundation for the realization of stress field visualization. In order to realize the data sharing in different formats, the data in a uniform format for the re-storage, analysis and processing was carried out.

1. Introduction

Along with the rapid development of technology, energy saving, high efficiency has become a new theme study (Rahimi et al., 2017). Known as the magnesium alloy structural material twenty-first century green engineering for its unique advantages and is widely used in magnesium alloy magnesium alloy matrix is by adding other metal elements, is a practical structural materials in the light, with a low density, high strength, high rigidity, shock absorption reduction characteristics good noise performance (Choobi and Haghpanahi, 2012). In addition, the magnesium alloy has bad corrosion resistance, anti radiation and electromagnetic shielding, recycling utilization rate of up to 100%; the stability is higher, and with good forming properties of die casting, magnesium alloy products wall thickness is less than 0.6mm, and the aluminum alloy is 1.2~1.5mm, so the car can be used all kinds of casting magnesium alloy (Yang and Shao, 2009). The rapid development of magnesium alloy is widely utilized at present, magnesium alloy, magnesium manganese alloy, mainly used in aviation, aerospace, automotive and 3C industries. However, restricted by the processing technology, equipment and price factors, the dosage of magnesium alloys is still far lower than steel and aluminum alloy (Lightfoot and McPherson, 2006). The advantages of the study of standard wrought magnesium alloy AZ80 has this kind of alloy, is the main material for the production of magnesium alloy automobile wheel hub at present. Study on the friction stir has important application value and practical significance of welding (Vilar and Zapata, 2009). Magnesium alloy is beyond all dispute many advantages, but its still exist many weaknesses. Led to the current aluminum alloy and steel market share is far higher than that of magnesium alloy products. There are several reasons (Yahia and Belhadj, 2011). The chemical characteristics of the magnesium alloy has a lively, easily oxidized combustion in air, lead smelting and processing is very difficult. Magnesium reacts with oxygen in the air to generate Magnesium Oxide is loose and porous, poor thermal conductivity. So it is in the melting magnesium alloy is particularly important when protection measures. So the production of magnesium alloy is difficult, the production cost is high, the production technology also is not mature. Low absolute strength of magnesium alloys, especially high temperature strength and high temperature creep resistance is poor. Its products are mainly concentrated in the magnesium steering wheel, engine bracket and the instrument panel and other structural parts, also rarely involve transmission parts, engine and other key components of high temperature. So it is very important for high temperature creep resistance of magnesium alloy. Close packed structure of magnesium of the six party, the room temperature plasticity is low, easy to brittle fracture. When the temperature is above 250 °C, Mg crystal slippage, strengthen the capability of plastic deformation. Friction stir welding (FSW)

is the most attract attention and the most development potential since the advent of laser welding technology of advanced welding technology, this welding method by British Welding Research Institute of C.J.Dwaes and W.M.Thomas et al in 1991 invented and patented it. Since FSW got pay close attention to industrial manufacturing field, this revolutionary connection technology has after get the scale in foreign manufacturing field (Martin et al., 2010).

2. The friction heat and flow model of friction stir process

2.1 Compression mold lubricant selection

FSW process temperature and stress field change is very complicated, using the direct thermal coupling method is difficult to handle loading a variable analysis problem and the analysis of temperature field in friction problem of mechanism transformation, and direct coupling speed have higher requirements for computer calculation, using stepwise coupling is flexible and practical the larger, so this paper will use the indirect coupling legal analysis (Lins et al., 2017; Liu et al., 2011). ANSYS in the use of the indirect method of thermal stress coupling analysis, the node temperature obtained will be used as body load in structural analysis of thermal analysis in the node temperature applied to have two kinds of choices the structural unit, the selection principle of structure model and thermal model is whether a similar grid. If the thermal structure the cells are the same node number, you can use the command will heat model is automatically converted to a corresponding structure model, directly from the thermal analysis results file will be applied to the structure model of temperature readout. But sometimes in order to get more good results, thermal and structural grids are not entirely consistent, then the ANSYS interpolation model of the structure node body load exceeds the thermal model, use the BFNIT command to thermal interpolation results (De et al., 2017).

The stirring head shape was shown in Figure 1, based on the tool shape, the total heat production welding process of G into Q_a , Yao, part of Q_c three, Q_b as the stirring head shoulder part of the heat generated, what solder pin outer cylinder part heat generation, Q_c welding needle end round face part of the heat generated, the total heat production of $Q_t=Q_a + Q_b + Q_c$.

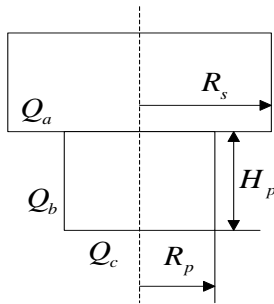


Figure 1: The stirring head shape

For welding needle end round face and micro shaft shoulder of the torus surface dA

$$dA = rd\theta dr \quad (1)$$

$$dQ_a = \omega r \tau dA = 2\pi n r^2 \tau_a d\theta dr$$

$$dQ_b = \omega r \tau dA = 2\pi n r^2 \tau_b d\theta dz \quad (2)$$

$$dQ_c = \omega r \tau dA = 2\pi n r^2 \tau_c d\theta dr$$

For the above three type in the corresponding in the contact surface integral:

$$Q_a = \int_0^{2\pi} \int_{R_p}^{R_s} \omega r^2 \tau_a dr d\theta = \frac{4}{3} \pi^2 \tau_a n (R_s^3 - R_p^3)$$

$$Q_b = \int_0^{2\pi} \int_0^{H_p} \omega r^2 \tau_b dz d\theta = 4\pi^2 \tau_b n R_p^2 H \quad (3)$$

$$Q_c = \int_0^{2\pi} \int_0^{R_p} \omega r^2 \tau_c dr d\theta = \frac{4}{3} \pi^2 \tau_c n R_p^3$$

Practical finite element analysis of deformation after welding, the value of relative the original finite element model is very small, direct image superimposed to obtain the deformation is not obvious, can well display the deformation law of weldments. Therefore, this paper in the design of welding deformation map, the introduction of the amplification coefficient of deformation, deformation value of amplification after added to the original model. Figure 2 are respectively welded components deformation map multiple after different amplification.

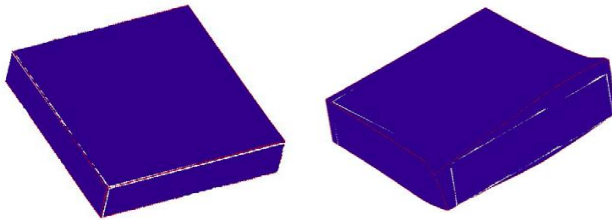


Figure 2: Welded components deformation map multiple after different amplification

2.2 The flow stress constitutive determine equation

Follow the first law of thermodynamics thermal analysis, the law of conservation of energy:
For a closed system (not the quality of the inflow or outflow):

$$Q - W = \Delta U + \Delta KE + \Delta PE \quad (4)$$

In the formula: Q---Quantity of heat; W---Work; ΔU ---Internal energy of the system; ΔKE ---Kinetic energy of the system; ΔPE ---Potential energy of system.

For the heat transfer problem in most engineering:

$$\Delta KE = \Delta PE = 0 \quad (5)$$

Generally considered not doing work:

$$W = 0, \text{ then: } Q = \Delta U \quad (6)$$

For the steady state thermal analysis:

$$Q = \Delta U = 0 \quad (7)$$

In engineering usually consider radiation between two or more than two objects, each object in a system while the radiation and absorption of heat. Heat transfer net between them can be used to calculate the Stephen Boltzmann equation:

$$q^s = \varepsilon \sigma A_1 F_{12} (T_1^4 - T_2^4) \quad (8)$$

Stress strain relationship is an important form of description of the mechanical properties of materials, through the German INSPEKTTABLE 100KN high temperature electronic universal material testing machine output is the engineering stress-strain curve. Need to be modified for the true relationship curves, and can be modified according to the following formula.

$$\varepsilon = \ln(1 + \varepsilon_1) \quad (9)$$

$$\sigma = \sigma_1(1 + \varepsilon_1) \quad (10)$$

In the formula: ε --- True strain, σ ---True stress(MPa), ε_1 --- Engineering strain, σ_1 ---Engineering stress(MPa).

2.3 Microstructure change before and after friction

In order to explain the friction phenomenon and its mechanism, the scientists put forward a variety of theories. When the contact the two surface occurs, when under load, some points of contact of rough large unit pressure micro convex body, plastic yielding and plastic deformation of asperities top. Occur in micro convex body top process of the plastic flow, two micro convex body close to each other, resulting in contact District new cause. Low stress condition, follow the exponential relationship between σP and Z:

$$\dot{\varepsilon} = A_1 \sigma^n \exp\left[\frac{-Q}{RT}\right] \quad (11)$$

Under high stress conditions, follow the exponential relationship between σ P and Z:

$$\dot{\varepsilon} = A_2 \exp(\beta\sigma) \exp\left[\frac{-Q}{RT}\right] \quad (12)$$

All stress state, follow a hyperbolic function of the relationship between σ P and Z:

$$\dot{\varepsilon} = A[\sinh(\alpha\sigma)]^n \exp\left[\frac{-Q}{RT}\right] \quad (13)$$

$$n = \frac{\beta}{\alpha} \quad (14)$$

In the formula: A--- Structure factor(s-1); σ --- Flow stress(MPa); n---Stress exponent; h---Strain values of corresponding flow stress σ ; The rest A1,n1,A2, α , β are bare temperature independent constant

3. Experimental Results

3.1 Experimental analysis

This paper selects eight node hexahedral elements for three-dimensional two unit, finite element calculation using the 2 * 2 * 2 Gauss integral. The welding temperature distribution at the same time was obtained in Figure 3.

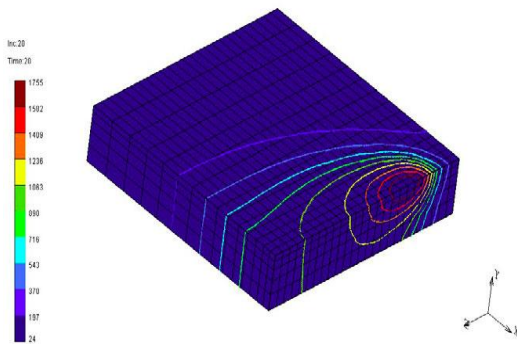


Figure 3: The welding temperature distribution at the same time obtained

The finite element results file directly, stored at the node temperature value, and then processing visualization graphics rendering, just as the node information display. Therefore, dealing with the analysis of welding temperature field after the direct extraction of nodes, data stored in the graphics display can be. Finite element stress analysis is the displacement as basic unknown quantity, to obtain the stress and strain values according to the displacement derivative. So the finite element results directly in the file stores a displacement node, but the stress calculation of finite element results in the nodes of the poor accuracy, storage finite element stress information form so with high precision element Gauss points results. But in engineering practice are often more concerned about the stress element edge and node, you must first through the interpolation calculation transformed into node on the results can be used for visual analysis of post processing.

The axial pressure of FSW make high-speed rotation of the stirring head shaft shoulder and welding pieces of the top surface of friction heat, with the heat accumulation, the temperature gradually increased, and the heat transfer to the below and in front, so that the moving resistance becomes smaller, and the stirring head moves forward along the weld direction, needle high speed rotating friction stir weld line the whole cross section of weld also friction heat and temperature rise. With the development of the whole cross section of weld temperature rises, achieve the reply, the grain growth. This process is heat treatment process on a heating. Figure 4 shows the plate welding isotherm distribution at a certain moment in the process.

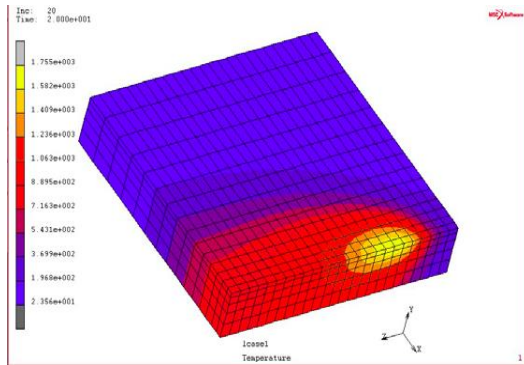


Figure 4: The plate welding isotherm distribution at a certain moment in the process

3.2 The experimental scheme

The basic idea of finite element method of continuous structure is divided into finite elements, and set the limited nodes in each unit, the continuum is seen as the only aggregate of a group of units connected at nodes; at the same time, the selected field function node value as the basic unknown quantity, and in each unit suppose an approximate interpolation function to represent the distribution unit midfielder function; then use some change in mechanics to establish for the finite element solution node unknown quantity equation principle, which will be a problem of infinite degree of freedom in the continuous domain into a finite degree of freedom problem in discrete domain. By solving and the whole assembly can unit the field function is determined by using the nodal solution of the value and the setting of interpolation function. The finite element calculation results can provide the distribution and change of temperature field is very rich information. Figure 5 is a 9 weld center Y direction ($Z=1.5\text{mm}$) temperature change curves of different points, heat source moving along the weld center line to the negative direction of Y axis, so each point in different speed of temperature rise stage, reaching the highest temperature time.

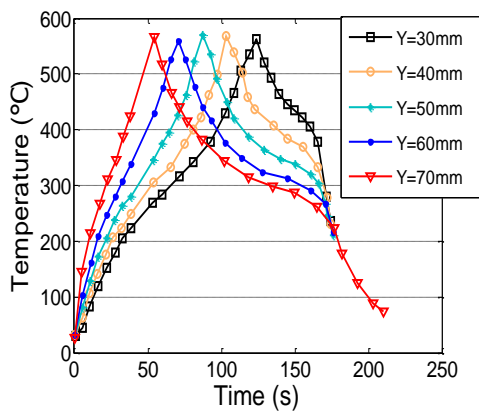


Figure 5: Nine weld center Y direction ($Z=1.5\text{mm}$) temperature change curves of different points

3.3 Processing analysis after FSW

Two pieces of $50\text{mm} \times 50\text{mm} \times 10\text{mm}$ steel plate welded into a tablet, does not open the mouth, without filler wire. Welding voltage, current are respectively 200V and 20A , the welding rate is 2mm/s , a commercial finite element software thermo mechanical coupling calculation of the welding process, welding temperature, should obtain relevant data of force and displacement field. In Figure 6, (a) said on the plane of symmetry X welding node displacement is zero, (b) three vertex nodes in the Y graph to the displacement is zero.

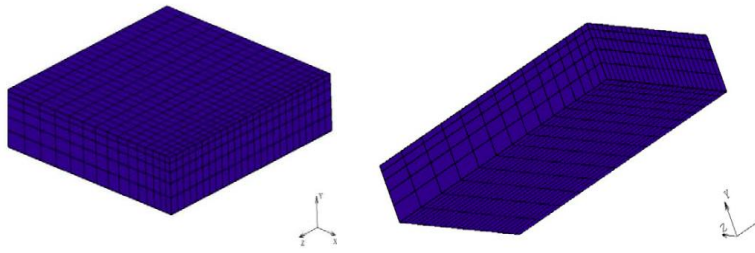


Figure 6: (a) the plane of symmetry X welding node, (b) three vertex nodes in the Y graph

4. Conclusions

Analysis technology of the treatment of finite element for the FSW process was studied after the FSW process. The finite element analysis, computer image processing technology, programming and software development technology in the integrated design of welding structure, finite element, eight nodes hexahedron unit support plate after treatment system. Welding of AZ80 magnesium alloy in friction during deformation, work hardening and dynamic softening occurred two processes. With the deformation degree of continue to increase, the dynamic recovery and more fully, so that further enhance the softening effect.

References

- Choobi M.S., Haghpanahi M., 2012, Prediction of welding-induced angular distortions in thin butt-welded plates using artificial neural networks, *Computational Materials Science*, 62, 152-159.
- De Caprariis B., De Filippis P., Hernandez A.D., Petruccio A., Scarsella M., Verdone N., 2017, Use of Low Cost Natural Materials for Tar Abatement Process, *Chemical Engineering Transactions*, 57, 91-96
- Lightfoot M.P., McPherson N.A., 2006, Artificial neural networks as an aid to steel plate distortion reduction, *Journal of Materials Processing Technology*, 172, 238-242.
- Lins J.M., Santos L., Santos V.A., Sarubbo L.A., 2017, Industrial Reuse of Water from Chemical Washing of Residual Frying Oil, *Chemical Engineering Transactions*, 57, 523-528
- Liu D., Nishio H., Nakata K., 2011, Anisotropic property of material arrangement in friction stir welding of dissimilar Mg alloys, *Materials & Design*, 32(10), 4818-4822.
- Martín Ó., Tiedra P.D., López M., 2010, Artificial neural networks for pitting potential prediction of resistance spot welding joints of aisi 304 austenitic stainless steel, *Corrosion Science*, 52(7), 2397-2402.
- Rahimi A.N., Mustafa M.F., Zaine M.Z., Ibrahim N., Ibrahim K.A., Hamid M.K.A., 2017, Hydrocarbon Mixture Fractionation Direct Sequence Retrofitting and Feed Condition Sensitivity Analysis, *Chemical Engineering Transactions*, 56, 787-792, DOI: 10.3303/CET1756132
- Vilar R., Zapata J., 2009, An automatic system of classification of weld defects in radiographic images, *NDT&E International*, 42(5), 467-476, DOI: 10.1784/insi.2010.52.3.134
- Yahia N.B., Belhadj T., 2011, Automatic detection of welding defects using radiography with a neural approach, *Procedia Engineering*, 10, 671-679, DOI: 10.1016/j.proeng.2011.04.112
- Yang H., Shao H., 2009, Distortion-oriented welding path optimization based on elastic net method and genetic algorithm, *Journal of Materials Processing Technology*, 209, 4407-4412, DOI: 10.1016/j.jmatprotec.2008.11.019